TCDMATH 05-04
HD-THEP-05-10

Doubly Periodic Instanton Zero Modes

C. Ford [a] and **J. M. Pawlowski** [b]

[a] *School of Mathematics*
Trinity College, Dublin 2, Ireland.
ford@maths.tcd.ie

[b] *Institut für Theoretische Physik,*
Universität Heidelberg, Philosophenweg 16
D 69120 Heidelberg, Germany.
J.Pawlowski@thphys.uni-heidelberg.de

Abstract

Fermionic zero modes associated with doubly periodic $SU(2)$ instantons of unit charge are considered. In cases where the action density exhibits two 'instanton cores' the zero mode peaks on one of four line-segments joining the two constituents. Which of the four possibilities is realised depends on the fermionic boundary conditions; doubly periodic, doubly anti-periodic or mixed.

In this Letter we consider fermionic zero modes for the recently discussed doubly periodic instantons [1, 2]. Two complementary constituent descriptions of these objects were provided; charge one instantons can be built out of two overlapping instanton cores *or* two static monopoles. Explicit computations show that in square tori the action density peaks at two points in $T^2 \times R^2$ in line with the core picture. For elongated tori with high aspect ratios the action density is concentrated in two tubes which can be interpreted as the worldlines of monopole constituents. The basic properties of these monopoles (separation and mass ratio) follow much the same pattern as found for the monopole constituents of calorons [3, 4, 5, 6]. Here we compute the zero mode density within a two-dimensional slice including the constituent locations for various boundary conditions. These results are compared with the action density calculations reported in refs. [1, 2]. Of particular

interest are the localisation properties of the zero modes with respect to the instanton core constituents and their evolution as the aspect ratio, or temperature, is increased.

To begin we recall some basic definitions regarding gauge fields on $T^2 \times R^2$. A doubly-periodic gauge potential is understood to be an anti-hermitian potential defined throughout R^4 which is periodic modulo gauge transformations U_1 and U_2 in two directions

$$\begin{aligned} A_\mu(x_0, x_1 + L_1, x_2, x_3) &= U_1 \left(A_\mu(x_0, x_1, x_2, x_3) + \partial_\mu\right) U_1^{-1}, \\ A_\mu(x_0, x_1, x_2 + L_2, x_3) &= U_2 \left(A_\mu(x_0, x_1, x_2, x_3) + \partial_\mu\right) U_2^{-1}. \end{aligned} \tag{1}$$

In general the transition functions U_1 and U_2 are x-dependent. However we will work in a gauge where they are constant commuting group elements. Then tr U_1 and tr U_2 are the two holonomies (assuming that A_1 and A_2 vanish at infinity). We specialise to self-dual $SU(2)$ potentials in the one-instanton sector. The Weyl operator

$$D^\dagger(A) = -\sigma_\mu^\dagger \left(\partial_\mu + A_\mu\right) \tag{2}$$

with $\sigma_\mu^\dagger = (1, -i\tau_1, -i\tau_2, -i\tau_3)$ and τ_i are Pauli matrices, is expected to have a single fermionic zero mode. To specify the periodicity properties of the fermionic zero mode two phases are required

$$\begin{aligned} \Psi(x_0, x_1 + L_1, x_2, x_3; z) &= e^{iz_1 L_1} U_1 \Psi(x_0, x_1, x_2, x_3; z) \\ \Psi(x_0, x_1, x_2 + L_2, x_3; z) &= e^{iz_2 L_2} U_2 \Psi(x_0, x_1, x_2, x_3; z). \end{aligned} \tag{3}$$

To make contact with the Nahm formalism the phases are parametrised by dimensionful coordinates z_1 and z_2 rather than angles; these have the interpretation as coordinates of the dual torus, $\tilde{T}^2$, since the replacements $z_1 \to z_1 + 2\pi/L_1$ $z_2 \to z_2 + 2\pi/L_2$ leave the boundary conditions unchanged. Such general boundary conditions have also been studied in a lattice context [7]. The choice $z_1 = z_2 = 0$ leads to periodic fermions while $z_1 = \pi/L_1$, $z_2 = \pi/L_2$ provides 'physical' anti-periodic solutions. Another interesting case is when z_1 and z_2 are correlated with the two holonomies.

The transition functions can be parametrised as follows

$$U_1 = e^{-i\omega_1 L_1 \tau_3}, \quad U_2 = e^{-i\omega_2 L_2 \tau_3}, \tag{4}$$

where $\omega = (\omega_1, \omega_2)$, like $z = (z_1, z_2)$, can be considered an element of the dual torus. Note that there is no charge-one instanton solution for trivial holonomy $\omega = 0$. Like R^4

instantons and calorons the $k = 1$ solution has a scale parameter, λ, which can be thought of as the instanton size. The scale parameter fixes another property of the instanton namely its *flux* κ; asymptotically the instanton has the form

$$A_\mu(x) \sim a_\mu(x_0, x_3)\tau_3, \tag{5}$$

where a_μ is a $U(1)$ self-dual potential in R^2. The flux is defined through

$$\kappa = \lim_{R\to\infty} \frac{i}{2\pi} \int_{C(R)} (a_0\ dx_0 + a_3\ dx_3)\,, \tag{6}$$

where $C(R)$ is a circle of radius R in the $x_0 - x_3$ plane. The sign of κ is ambiguous since the signs of the a_μ can be flipped via a constant gauge transformation (a Weyl reflection). Moreover, we may assume that κ lies between 0 and 1 since κ can be changed by an integer amount via a smooth gauge transformation. The asymptotic flux can also have non-zero components in the compact x_1 and x_2 directions, i.e. a_1 and a_2 need not be zero. When $a_1 = a_2 = 0$ the instanton has a radial symmetry; the action density depends on x_1, x_2 and $r = \sqrt{x_0^2 + x_3^2}$ only. In this case the action density decays exponentially and there is a simple relation between the scale parameter λ and the flux

$$\kappa = \frac{\pi\lambda^2}{L_1 L_2}. \tag{7}$$

These special radial solutions have seven parameters; the flux κ (or equivalently the size λ) the two holonomies and four translations in $T^2 \times R^2$. Together the $\kappa \to -\kappa$ ambiguity and the $\kappa \equiv \kappa + 1$ equivalence imply that the fluxes κ and $1-\kappa$ are physically indistinguishable. This gives two possible instanton sizes $\lambda_1 = \sqrt{\kappa L_1 L_2/\pi}$ and $\lambda_2 = \sqrt{(1-\kappa)L_1 L_2/\pi}$. In [1] it was argued that the instanton possesses two *instanton core* constituents with sizes λ_1 and λ_2. Taking $x_\mu = 0$ as the position of the first core the second is centred at $x_1 = L_1 L_2 \omega_2/\pi$, $x_2 = -L_1 L_2 \omega_1/\pi$, $x_0 = x_3 = 0$, i.e. the core separation is fixed by the holonomies. For square tori ($L_1 = L_2$) explicit calculations of the action density clearly show two instanton-like peaks at the expected locations.

In the special case $\kappa = \frac{1}{2}$ the two cores are identical. Here the flux can be interpreted as a center vortex. These solutions are decompactified four torus instantons of unit charge (the $L_0, L_3 \to \infty$ limit of an $SU(2)$ instanton on T^4 with periods L_0, L_1, L_2 and L_3). The center vortex is a remnant of a torus twist, $Z_{03} = -\mathbb{1}$, see ref. [8]. Because of the exponential

decay, the $\kappa = \frac{1}{2}$ solutions are expected to approximate four torus instantons with large but finite L_0 and L_3 extremely well (see also [9]). These doubly periodic instantons can be seen as the opposite extreme to 't Hooft's constant curvature solutions which exist when $L_1 L_2 = 2 L_0 L_3$. An analytic interpolation between these two regimes is still lacking (see however [10]). In the absence of analytic solutions a constituent description (in terms of cores, monopoles or otherwise) as well as information concerning the moduli-spaces and their metrics would represent a considerable advance.

If one period is much larger than the other, say $L_1 >> L_2$, the core picture fails; the action density is concentrated around two monopole worldlines. These monopole constituents follow a similar pattern to that observed for charge one calorons; ω_2 determines the mass ratio of the two monopoles and their spatial separation is $\pi\lambda^2/L_2 = \kappa L_1$. The caloron zero mode [11] localises to one of the monopole constituents according to the value of z. As z passes through a critical value (where z is correlated with the holonomy) the zero mode switches its support to the other monopole. If z is exactly at a critical value the zero mode peaks at both monopole locations. Furthermore these delocalised zero modes do not decay exponentially (the decay is sufficiently fast to give a normalisable solution). In the doubly periodic case we have to distinguish between the core ($L_1 \approx L_2$) and monopole ($L_1 >> L_2$ or $L_2 >> L_1$) regimes. If $L_1 >> L_2$ the fermionic zero mode is expected to be caloron-like in that it will localise to one monopole for $-\omega_2 < z_2 < \omega_2$ and the other for $\omega_2 < z_2 < -\omega_2 + 2\pi/L_2$. If $z_2 = \pm\omega_2$ the zero mode will see both monopoles (assuming $z_1 \neq \pm\omega_1$, since as we shall argue $(z_1, z_2) = \pm(\omega_1, \omega_2)$ are *very* special cases). What is less obvious is how the zero mode behaves in the core regime. We have computed the zero mode density $\Psi^\dagger(x;z)\Psi(x;z)$ within the two-dimensional slice $x_0 = x_3 = 0$ for various choices of κ, ω and z. When $L_1 = L_2$, the zero mode localises to one of four lines joining the cores.

Consider the case $L_1 = L_2 = 1$, $\kappa = \frac{1}{2}$, $\omega_1 = \omega_2 = \frac{1}{2}\pi$. Here the two (equal sized) cores are particularly well resolved in the action density. They are located at the origin $(x_1, x_2) = (0, 0)$, and in the centre of the torus $(x_1, x_2) = (\frac{1}{2}, \frac{1}{2})$. For $z_1 = z_2 = \pi$, the physical anti-periodic case, the zero mode is not localised on a single core but smeared around a line-segment joining the core at the corner $(x_1, x_2) = (0, 1)$ and core in the middle of the torus $(x_1, x_2) = (\frac{1}{2}, \frac{1}{2})$, see the left plot in figure 1.

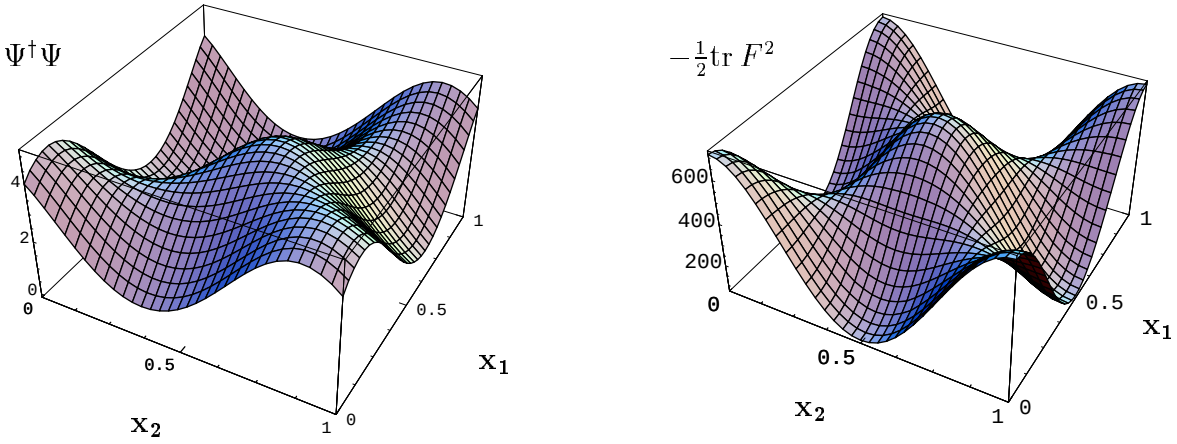

Figure 1: zero mode density $\Psi^\dagger\Psi$ and action density $-\frac{1}{2}\mathrm{tr}F^2$ for $x_\perp = 0$, $\kappa = \frac{1}{2}$, $\omega = \frac{\pi}{2}(1,1)$ and $z = \pi(1,1)$ (anti-periodic).

Taking instead $z = 0$, the periodic case, yields a similar line-localisation but with a different pairing arrangement; it stretches between the core in the middle and that at $(x_1, x_2) = (1, 0)$, see the left plot in figure 2.

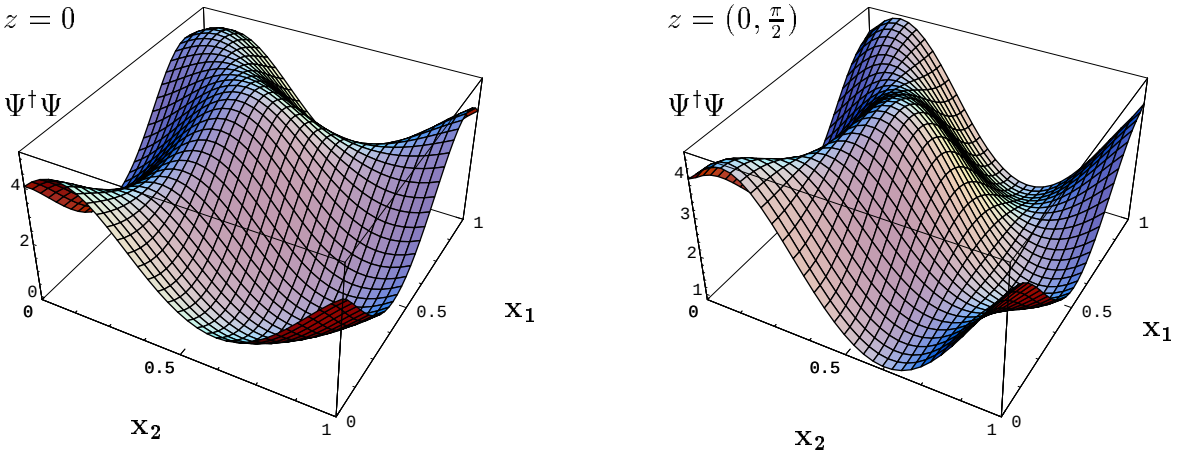

Figure 2: zero mode density $\Psi^\dagger\Psi$ for $x_\perp = 0$, $\kappa = \frac{1}{2}$ and $z = (0, 0)$ (periodic) and $z = (0, \frac{\pi}{2})$ (periodic in x_1 and anti-periodic in $2x_2$).

The zero modes densities in figures 1 and 2 (left plots) can be mapped into each other by a 180 degree rotation. The other two pairing arrangements are given by $z = (0, \pi)$, where the zero mode stretches between the cores at $(x_1, x_2) = (0, 0)$ and $(x_1, x_2) = (\frac{1}{2}, \frac{1}{2})$ and $z = (\pi, 0)$, where the zero mode stretches between the cores at $(x_1, x_2) = (1, 1)$ and $(x_1, x_2) = (\frac{1}{2}, \frac{1}{2})$. The transition between two of the four possible arrangements is a smooth

one. For example, taking $z = (0, \pi/2)$ generates a superposition of two of the four generic pairings, namely between $z = (0, \pi)$ and $z = (0, 0)$, see the right plot in figure 2.

The transition from the above situation to the finite temperature case is accessed by increasing L_1 (or L_2) starting from $L_1 = L_2$. This was done in [2] for the action density showing the crossover from instanton cores to monopole constituents. In figure 3 we show the corresponding zero mode densities for zero modes with anti-periodic boundary conditions, and aspect ratios $a = L_1/L_2 = \frac{3}{2}, 2, 3$.

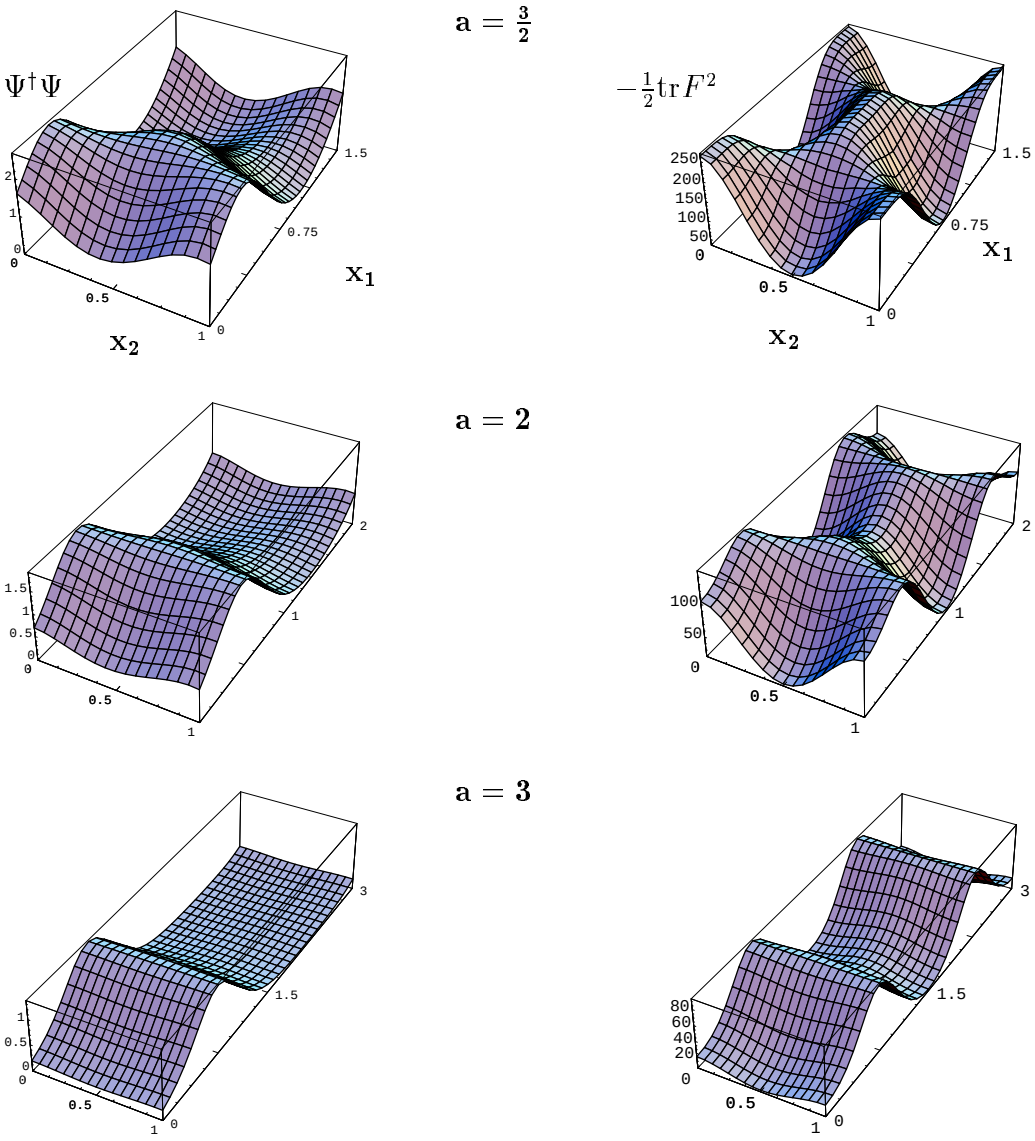

Figure 3: zero mode density $\Psi^\dagger\Psi$ for $x_\perp = 0$ $\kappa = \frac{1}{2}$ and $\omega = \frac{\pi}{2}(a^{-1}, 1)$ and $a = \frac{3}{2}, 2, 3$ (anti-periodic)

The equal length case $a = 1$ is already shown in figure 1. If $a > 1$ the zero mode peaks at one of the monopole worldlines. In fact the monopole structure emerges in the zero modes *before* it is visible in the action density; the $a = \frac{3}{2}$ zero mode already has some resemblance to the large a monopole like regime whereas (stretched) cores are still visible in the action density. In figure 4 we show zero mode and action densities for the case $\kappa = \frac{5}{8}$. In the $a = 1$ core regime the zero mode density peaks at the smaller core but one still can see a preferred line joining the smaller core at the centre to the larger core at the corner $(x_1, x_2) = (0, 1)$. Here the evolution to the monopole regime is slower due to the presence of a smaller core. But as with the $\kappa = \frac{1}{2}$ case the monopole structure appears in the zero mode density before it can be seen in the action density.

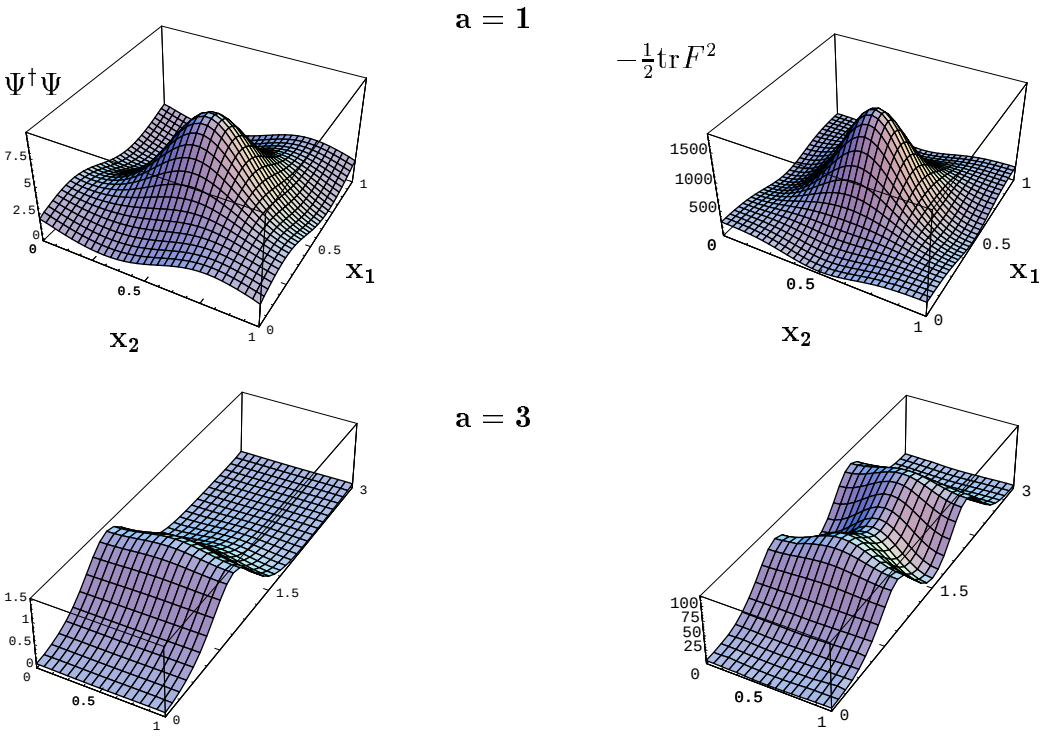

Figure 4: zero mode density $\Psi^\dagger\Psi$ for $x_\perp = 0$, $\kappa = \frac{5}{8}$ and $\omega = \frac{\pi}{2}(a^{-1}, 1)$ and $a = 1, 3$ (anti-periodic)

A further interesting case concerns the limit where z approaches $\pm\omega$. If $\kappa \neq \frac{1}{2}$ the zero mode does localise to a single core as z *approaches* ω or $-\omega$. However *at* $z = \omega$ the zero mode is not normalisable. If $\Psi(x, z)$ is normalised then for a fixed x it tends to zero as z

tends to ω. When $\kappa = \frac{1}{2}$ the zero mode also becomes non-normalisable as z approaches ω but during the approach the pair structure survives, i.e. however close z is to ω the zero mode will not be localised to a single core. When $z = \omega$ the equation $D^\dagger \Psi = 0$ has two solutions $\Psi^I(x)$ and $\Psi^{II}(x)$ which are supported at the first and second core, respectively. These 'zero modes' are smooth but not normalisable. Like the $z = \omega$ caloron zero mode they decay algebraically - but not fast enough to be normalisable. As z approaches ω the zero mode has the form

$$\Psi(x;z) \sim |z-\omega|^{\kappa} \Psi^I(x) + |z-\omega|^{-\kappa}(z_1 + iz_2 - \omega_1 - i\omega_2)\Psi^{II}(x). \tag{8}$$

As z approaches ω the Ψ^{II} contribution is suppressed if $\kappa < \frac{1}{2}$ and for $\kappa > \frac{1}{2}$ the first term is suppressed. Accordingly, the zero mode is localised at the smaller core. If $\kappa = \frac{1}{2}$ neither core is favoured and the pair localisation persists. Note that the zero mode density depends on the phase of $z_1 + iz_2 - \omega_1 - i\omega_2$ so that the form of $\Psi^\dagger\Psi$ for $z \sim \omega$ depends on the direction of approach to ω. This is why all four pairings can be seen in the $z \to \omega$ limit when $\kappa = \frac{1}{2}$.

The plots presented in this Letter were generated using an explicit formula for $\Psi(x;z)$ valid in the two-dimensional slice $x_0 = x_3 = 0$. To conclude we outline the derivation of this formula. The construction hinges on the fact that the $SU(2)$ gauge potential, $A_\mu(x)$, has a simple abelian Nahm transform, $\hat{A}(z)$, with components [2]

$$\hat{A}_1(z) = -i\partial_{z_2}\phi(z), \quad \hat{A}_2(z) = i\partial_{z_1}\phi(z), \quad \hat{A}_0(z) = \hat{A}_3(z) = 0, \tag{9}$$

where $\phi(z)$ is doubly-periodic and harmonic except at two flux singularities in $\tilde{T}^2$. This is the form of the Nahm potential associated with radially symmetric one instantons on $T^2 \times R^2$. In the non-radial case, which we do not consider here, $\hat{A}_0$ and $\hat{A}_3$ are non-zero (see also [12]). The instanton can be expressed as a Nahm transform of $\hat{A}(z)$:

$$A_\mu^{pq}(x) = \int_{\tilde{T}^2} d^2z \; \psi^{p\,\dagger}(z;x) \frac{\partial}{\partial x^\mu} \psi^q(z;x), \tag{10}$$

where $\psi^p(z;x)$ $(p = 1, 2)$ are orthonormal and periodic (with respect to $z_1 \to z_1 + 2\pi/L_1$ and $z_2 \to z_2 + 2\pi/L_2$) zero modes of the Weyl operator

$$D_x^\dagger(\hat{A}) = -\sigma_\mu^\dagger D_x^\mu(\hat{A}), \tag{11}$$

where $D_x^\mu(\hat{A}) = \partial/\partial z_\mu + \hat{A}_\mu(z) - ix_\mu$ for $\mu = 1,2$ and $D_x^\mu(\hat{A}) = \hat{A}_\mu(z) - ix_\mu$ for $\mu = 0,3$. The Nahm zero modes can be written in the form

$$\psi^1(z;x) = D_x(\hat{A}) \begin{pmatrix} \varphi^{(1)}(z;x) \\ 0 \end{pmatrix}, \qquad \psi^2(z;x) = D_x(\hat{A}) \begin{pmatrix} 0 \\ \varphi^{(2)}(z;x) \end{pmatrix}, \tag{12}$$

where the $\varphi^{(p)}$ are specific singular solutions of the $\tilde{T}^2$ Laplace equation

$$\left(D_x^\mu(\hat{A})\right)^2 \varphi(z;x) = 0. \tag{13}$$

The fermionic zero mode $\Psi(x;z)$ can be written in a similar fashion to the Nahm zero modes

$$\Psi(x;z) = D(A) \begin{pmatrix} \Phi^{(1)}(x;z) \\ 0 \end{pmatrix} = D(A) \begin{pmatrix} 0 \\ \Phi^{(2)}(x;z) \end{pmatrix}, \tag{14}$$

where $\Phi^{(1)}$ and $\Phi^{(2)}$ are specific singular solutions of the $T^2 \times R^2$ Laplace equation

$$\left(\frac{\partial}{\partial x_\mu} + A_\mu(x)\right)^2 \Phi(x;z) = 0. \tag{15}$$

In fact, *one* of the components of $\Phi^{(p)}$ is $\varphi^{(p)}$

$$\Phi^{(1)}(x;z) = \begin{pmatrix} \tilde{\varphi}^{(1)}(z;x) \\ \varphi^{(1)}(z;x) \end{pmatrix}, \qquad \Phi^{(2)}(x;z) = \begin{pmatrix} \varphi^{(2)}(z;x) \\ \tilde{\varphi}^{(2)}(z;x) \end{pmatrix}. \tag{16}$$

The other components, $\tilde{\varphi}^{(1)}$ and $\tilde{\varphi}^{(2)}$, can be obtained from the requirement that $\Phi^{(1)}$ and $\Phi^{(2)}$ generate the same zero mode, i.e. equation (14). This requirement amounts to four first order PDEs for $\tilde{\varphi}^{(1)}$ and $\tilde{\varphi}^{(2)}$. The integrability condition for these equations can be expressed as another Laplace-type equation

$$\left(\frac{\partial}{\partial x_\mu} + A_\mu^B(x)\right)^2 \begin{pmatrix} \varphi^{(1)}(z;x) \\ \varphi^{(2)}(z;x) \end{pmatrix} = 0, \tag{17}$$

where $A_\mu^B(x)$ is an $SU(1,1)$ self-dual potential which is related to $A_\mu(x)$ by a simple Bäcklund-type transformation; more details of this structure will be given elsewhere.

The Nahm zero modes (12) lead to an instanton potential

$$\begin{aligned} A_{x_{||}} &= -\frac{\tau_3}{2}\partial_{x_{||}}\log\rho - 2\pi i(\tau_1 - i\tau_2)\kappa\rho\partial_{\bar{x}_\perp}\frac{\nu^*}{\rho} \\ A_{x_\perp} &= -\frac{\tau_3}{2}\partial_{x_\perp}\log\rho + 2\pi i(\tau_1 - i\tau_2)\kappa\rho\partial_{\bar{x}_{||}}\frac{\nu^*}{\rho}, \end{aligned} \tag{18}$$

and $A_{\bar{x}_{||}} = -A^\dagger_{x_{||}}$, $A_{\bar{x}_\perp} = -A^\dagger_{x_\perp}$, where $\rho(x)$ is real and periodic and $\nu(x)$ is complex and periodic up to a constant phase. Here we have used two sets of complex coordinates for $T^2 \times R^2$; in the compact directions $x_{||} = x_1 + ix_2$, $\bar{x}_{||} = x_1 - ix_2$, and in the transverse non-compact directions $x_\perp = x_0 + ix_3$, $\bar{x}_\perp = x_0 - ix_3$. Derivatives and potentials are defined as $\partial_{x_{||}} = \frac{1}{2}(\partial_{x_1} - i\partial_{x_2})$, $A_{x_{||}} = \frac{1}{2}(A_1 - iA_2)$ and similarly for the other coordinates. Inserting (18) into (14) one can express the components of $\Psi(x;z)$ without reference to the $\tilde{\varphi}^{(p)}$. Two components are obtained using the $\Phi^{(2)}$ representation

$$\Psi_{11} = 2i\sqrt{\rho}\partial_{x_{||}}\frac{\varphi^{(2)}}{\sqrt{\rho}}, \qquad \Psi_{21} = 2\sqrt{\rho}\partial_{x_\perp}\frac{\varphi^{(2)}}{\sqrt{\rho}}, \tag{19}$$

and the remaining two components derive from the $\Phi^{(1)}$ representation

$$\Psi_{12} = 2\sqrt{\rho}\partial_{\bar{x}_\perp}\frac{\varphi^{(1)}}{\sqrt{\rho}}, \qquad \Psi_{22} = 2i\sqrt{\rho}\partial_{\bar{x}_{||}}\frac{\varphi^{(1)}}{\sqrt{\rho}}. \tag{20}$$

Here we have written the zero mode components $\Psi_{\alpha p}$ where α is a spinor index and p an $SU(2)$ color index. The representation of the caloron zero mode given in [11] has the same derivative structure. The fermionic zero mode given here has the normalisation

$$\int_{T^2\times R^2} d^4x\ \Psi^\dagger(x;z)\Psi(x;z) = 4L_1L_2, \tag{21}$$

and so the normalised zero mode density is

$$\Psi^\dagger\Psi = \frac{\rho}{L_1L_2}\left(\left|\partial_{\bar{x}_{||}}\frac{\varphi^{(1)}}{\sqrt{\rho}}\right|^2 + \left|\partial_{x_{||}}\frac{\varphi^{(2)}}{\sqrt{\rho}}\right|^2 + \left|\partial_{\bar{x}_\perp}\frac{\varphi^{(1)}}{\sqrt{\rho}}\right|^2 + \left|\partial_{x_\perp}\frac{\varphi^{(2)}}{\sqrt{\rho}}\right|^2\right). \tag{22}$$

We have written $A_\mu(x)$, $\psi^{(p)}(z;x)$ and $\Psi(x;z)$ in terms of the auxiliary objects $\rho(x)$, $\nu(x)$ and $\varphi^{(p)}(z;x)$. These can be expressed in terms of contributions to the inverse of $D^\dagger_x(\hat{A})D_x(\hat{A})$ which has the form [2]

$$\begin{aligned} &\left(D^\dagger_x(\hat{A})D_x(\hat{A})\right)^{-1}(z,z') \\ &\quad = \tfrac{1}{2}(\sigma_0 + i\sigma_3)e^{-\phi(z)}K_+(z,z';x)e^{-\phi(z')} + \tfrac{1}{2}(\sigma_0 - i\sigma_3)e^{\phi(z)}K_-(z,z';x)e^{\phi(z')}. \end{aligned} \tag{23}$$

The key formulae are

$$\rho(x) = K_+(-\omega, -\omega; x) = K_-(\omega, \omega; x), \qquad \nu(x) = K_+(\omega, -\omega; x), \tag{24}$$

and

$$\varphi^{(1)}(z; x) = e^{\phi(z)} \frac{K_-(z, \omega; x)}{\sqrt{\rho}}, \qquad \varphi^{(2)}(z; x) = e^{-\phi(z)} \frac{K_+(z, -\omega; x)}{\sqrt{\rho}}. \tag{25}$$

In [2] explicit forms for the $K_\pm$ functions were given for the two dimensional slice $x_\perp = 0$. Although the zero mode formulae involves $x_\perp$-derivatives they do not contribute if $x_\perp = 0$.

Using (19) and (20) the components of the smooth non-normalisable zero modes $\Psi^I(x)$ and $\Psi^{II}(x)$ can be recovered. For $\kappa < \frac{1}{2}$ and z close to ω, $\Psi(x; z) \sim |z - \omega|^\kappa \Psi^I(x)$ where

$$\Psi^I_{11} = 2ic\sqrt{\rho}\partial_{x_{||}} \frac{\nu}{\rho}, \qquad \Psi^I_{21} = 2c\sqrt{\rho}\partial_{x_\perp} \frac{\nu}{\rho}, \qquad \Psi^I_{12} = \frac{c\sqrt{\rho}}{2\pi\kappa}\partial_{\bar{x}_\perp} \frac{1}{\rho}, \qquad \Psi^I_{22} = \frac{ic\sqrt{\rho}}{2\pi\kappa}\partial_{\bar{x}_{||}} \frac{1}{\rho}, \tag{26}$$

where c is defined by $e^{-\phi(z)} \sim c|z - \omega|^\kappa$ for z close to ω. For large $|x_\perp|$ we have [2] $\rho \propto |x_\perp|^{-2\kappa}$ (ν decays exponentially) implying that $\Psi^{I\dagger}\Psi^I \propto |x_\perp|^{2(\kappa-1)}$ which is indeed too slowly decaying to normalise the solution.

Acknowledgements

We are grateful to DIAS, Dublin and the Institute for Theoretical Physics, University Tübingen for kind hospitality. This work has been supported by a grant from the Ministry of Science, Research and the Arts of Baden-Württemberg (Az: 24-7532.23-19-18/1) and the DFG under contract GI328/1-2.

References

[1] C. Ford and J. M. Pawlowski, Phys. Lett. B **540** (2002) 153 [hep-th/0205116].

[2] C. Ford and J. M. Pawlowski, Phys. Rev. D **69** (2004) 065006 [hep-th/0302117].

[3] W. Nahm, BONN-HE-83-16 *Presented at 12th Colloq. on Group Theoretical Methods in Physics, Trieste, Italy, Sep 5-10, 1983.*

[4] K. M. Lee and C. h. Lu, Phys. Rev. D **58** (1998) 025011 [hep-th/9802108].

[5] T. C. Kraan and P. van Baal, Nucl. Phys. B **533** (1998) 627 [hep-th/9805168].

[6] F. Bruckmann and P. van Baal, Nucl. Phys. B **645** (2002) 105 [hep-th/0209010].

[7] C. Gattringer and S. Solbrig, hep-lat/0410040;
C. Gattringer and R. Pullirsch, Phys. Rev. D **69** (2004) 094510 [hep-lat/0402008].

[8] G. 't Hooft, Commun. Math. Phys. **81** (1981) 267.

[9] A. Gonzalez-Arroyo and A. Montero, Phys. Lett. B **442** (1998) 273 [hep-th/9809037].

[10] M. Garcia Perez, A. Gonzalez-Arroyo and C. Pena, JHEP **0009** (2000) 033 [hep-th/0007113].

[11] M. Garcia Perez, A. Gonzalez-Arroyo, C. Pena and P. van Baal, Phys. Rev. D **60** (1999) 031901 [hep-th/9905016].

[12] M. Jardim, Commun. Math. Phys. **216** (2001) 1 [math.dg/9909069];
I. Frenkel and M. Jardim, Commun. Math. Phys. **237** (2003) 471 [math.qa/0205118].